



Corresponding Author:
Nguyen Huynh Duy Khang

Department of Electrical and Electronic Engineering, Tokyo Institute of Technology, Japan

Email: nguyen.h.ai@m.titech.ac.jp

Nguyen Huynh Duy Khang received bachelor degree in physics from Ho Chi Minh City University of Education in 2013, master degree in Radio Physics and Electronics from Ho Chi Minh City University of Science in 2015, and Ph.D. in Electrical and Electronic Engineering from Tokyo Institute of Technology in 2019. He is currently a JSPS Postdoctoral Research Fellow at Department of Electrical and Electronic Engineering, Tokyo Institute of Technology. His research focuses on spin-related transport phenomena in BiSb topological insulator and its application to spintronic devices.

<https://doi.org/10.15625/vap.2021.0006>

Giant spin-dependent phenomena in BiSb topological insulator – ferromagnet heterostructures

Nguyen Huynh Duy Khang¹ and Pham Nam Hai²

¹JSPS Postdoctoral Fellow, Department of Electrical and Electronic Engineering, Tokyo Institute of Technology, Japan and Lecturer, Department of Physics, Ho Chi Minh city University of Education, Vietnam

²Associate Professor, Department of Electrical and Electronic Engineering, Tokyo Institute of Technology and visiting Associate Professor, Center for Spintronics Research Network (CSRN), The University of Tokyo, Japan

ABSTRACT:

We review novel spin – related phenomena originating from the topological surface states in BiSb topological insulator/ferromagnet heterostructures, and discuss their applications to various spintronic devices, such as spin-orbit torque magnetoresistive random-access memory, racetrack memory, and skyrmion memory.

Keywords: *spin-orbitronics, topological insulator, BiSb*

1. From spintronics to spin-orbitronics

Just two decades ago, “desktops” or “personal computers” were very luxury terms. Today, they have become very popular and an irrevocable part of our lives, but partly replaced by mobile devices such as smartphone or notebook. From the introduction of transistor, which was invented in 1947 by J. Barden, W. Shockley and W. Brattain [1], the early progress of computing technology coincides with the development of integrated circuits based on CMOS technology that leads to the Digital Revolution. The number of transistors that can be integrated is double every 18 months, as predicted by G. Moore, and known as the Moore’s law [2]. The continuous device engineering has reduced the size of transistors down to few nanometers, getting closer to the end of the Moore’s law. As the consequence, the concept of electron’s transportation has begun to pose problems, and simply packing more transistors into the same area to improve performance has become very challenging and expensive. In addition, leakage current drastically increases at nano-scale, resulting in large idling power consumption. To continuously improve performance of electronic devices without further miniaturization, spintronics comes into play.

Spintronics or spin electronics is a new technology that utilizes the electrons’ intrinsic angular momentum, spin. Its concept is described in Fig. 1(a) as the overlap between electronic engineering (electric charge) and magnetic engineering (spin). Indeed, mass data storage technology, such as hard disk drives (HDDs), has used advanced spintronic magnetic sensors for read out from the 1990s. The capability of spintronic is being expanded to new generation of devices, such as magnetoresistive random access memory (MRAM) that exhibits unique advantages of low power consumption, non-volatility and high speed [4-5]. In MRAM, instead of using the

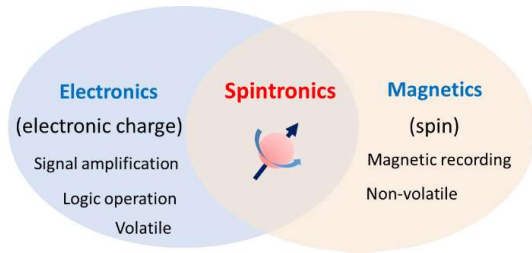


Figure 1. Concept of spintronics

“existence” or “absence” of electric charge, “0” and “1” binary data can be expressed by up-spin (\uparrow) or down-spin (\downarrow). Figure 2 illustrates an important concept in spintronics, the spin current. The flow of electrons will be merely a charge current, if their spins are mixed up and cannot be distinguished (Fig. 2(a)). However, there are situations where one spin population is larger than the other. Figure 2(b) illustrates this kind of circumstance where the density of spin-up electrons is higher than that of spin-down electrons. In this case, the charge current is accompanied by a spin current, thus called “spin-polarized current”. The net spin current is given by the spin-up current minus the spin-down current. Figure 2(c) shows a special case of spin current where the spin-up current and the spin-down current flows to opposite direction. Interestingly, in this situation, the charge current, which is the total of spin-up current and spin-down current, is zero. In contrast, there is a net spin current called “pure spin current”, which poses new ideas about generating a spin current without a charge current [6].

Once of the most important technology development in spintronics is MRAM. This type of memory is very promising for memory applications in general. Unlike dynamic random-access memory (DRAM) or static random-access memory (SRAM) whose data will be lost without power supply (volatile memories), MRAM stores data in magnetic materials and does not need power to maintain data. The first generation of MRAM is toggle MRAM, and its mechanism is visualized in Fig. 3(a). The storage elements of MRAM are magnetic tunnel junctions (MTJs), which are formed by two magnetic layers (a free layer and a fixed layer) separated by a thin insulating layer. Each data bit is recorded in the magnetic states of the MTJs,

depending on the relative direction between magnetization of the free and fixed layer (parallel or anti-parallel). The writing process is based on Oersted magnetic fields generated by nearby writing currents, while the reading process is performed by measuring the tunneling resistance between the two magnetic layers, which is high in anti-parallel and low in parallel magnetic configuration, a phenomenon called “tunneling magnetoresistance effect”.

The next generation of MRAM utilizes a new writing technique that does not require a magnetic field, proposed by Slonczewski and Berger [7-9]. They predicted that a spin polarized current can be generated by passing a charge current through the magnetic fixed layer. When this spin polarized current is injected to the magnetic free layer, it can generate a spin torque on the free layer for magnetization switching. This phenomenon is named as the spin-transfer torque (STT) with very promising implications, and experimentally demonstrated [10-12]. As illustrated in Fig. 3(b), when a charge current is passed through the MTJ, the spin polarized current from the fixed layer can switch the magnetization of the free layer.

STT-MRAM shows higher bit density which can reach Gbits storage capacity with lower operation power than that of toggle MRAM (only 4 Mbit chip for commercial product). As shown in Fig. 4(a), STT-MRAM has better scalability, and can possibility fill the memory gap between SRAM, DRAM, and NAND. However, the writing current and writing energy of MRAM are still too high and worse than SRAM or DRAM by one order of magnitude. Furthermore, the large writing current can lead to breakdown of the oxide tunneling barrier layer. The read disturbance or accident switching of the magnetic states can also happen. In addition, high writing current requires large driving transistors, which makes it difficult to further increase the bit density of MRAM to 10 Gbits [16].

Therefore, shorter write latency, lower power consumption, and higher density are required for the next generation of MRAM. As the results, spintronics

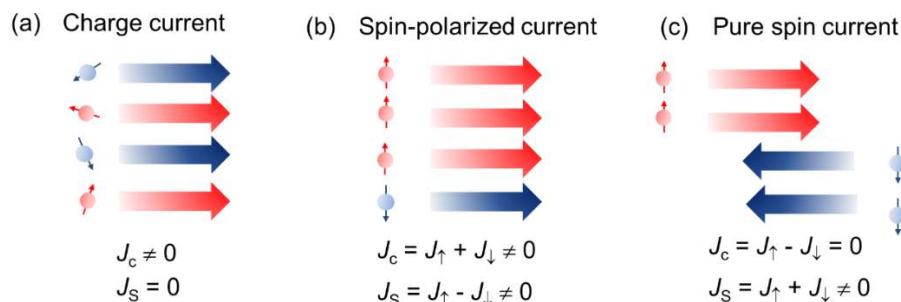


Figure 2. Schematic illustrations of (a) charge current, (b) spin-polarized current and (c) pure spin current.

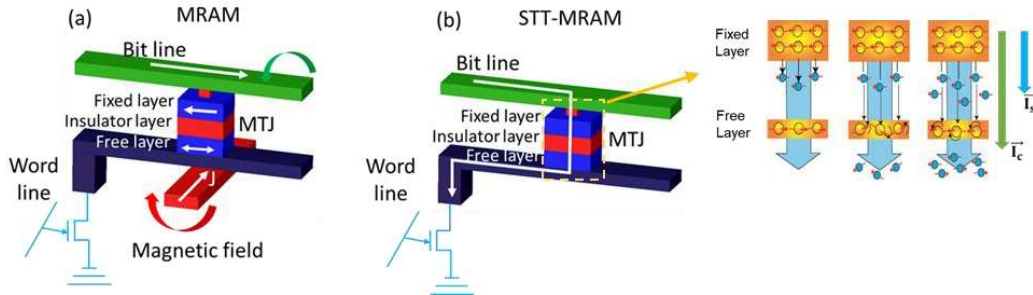


Figure 3. (a) Schematic illustration of the writing process in toggle MRAM. (b) Schematic illustration of the writing process in spin-transfer-torque (STT) MRAM. STT mechanism is shown in the right-hand side figure, for magnetization switching, where a spin-polarized current I_s , generated by passing a charge current I_c through the fixed layer, is injected to the free layer and generates a spin torque on the free layer

research has been gradually shifted toward the spin Hall effect originated from spin-orbit interaction (SOI) or spin-orbit coupling, which can generate a pure spin current more efficiently and reduce the writing current in MRAM.

2. SOT-MRAM – The next generation of MRAM

So far, spin-polarized current has been generated by passing a charge current through a ferromagnetic layer. However, the charge-to-spin conversion efficiency is limited by the maximum spin polarization $P = 1$ of the ferromagnetic layer. Recently, the spin Hall effect has emerged as a new way to generate pure spin currents with improved charge-to-spin conversion efficiency [13-15]. The pure spin current can be injected to the magnetic free layer for switching. This type of MRAM is called spin-orbit torque (SOT)-MRAM, and has emerged as a promising candidate that can overcome the disadvantages of STT-MRAM. In SOT-MRAM, a non-magnetic layer with strong spin Hall effect is in contact with the free magnetic layer. As illustrated in Fig. 5(b), a charge current flowing in the spin Hall layer can generate a pure spin current perpendicular to the interface by the spin Hall effect. This pure spin current can exert a spin torque (so called spin-orbit torque) on the free layer and switch its magnetization. The pure spin current density generated by a charge

current density J_c in the spin Hall layer is given by $J_s = (\hbar/2e)\theta_{SH} J_c$, where θ_{SH} is the charge-to-spin conversion efficiency or spin Hall angle [16-18].

Moreover, because the spin polarization direction of the pure spin current in SOT-MRAM is perpendicular to the magnetization, the spin-torque is maximized and the writing speed of SOT-MRAM can be as fast as 300 ps, compared with about 10 ns in STT-MRAM [8]. Thus, by reducing both the writing current and the writing time, SOT-MRAM can significantly lower the writing energy. Moreover, the writing current does not flow through the MTJ in the writing process, thereby MTJ's reliability can be drastically improved. Finally, if we can reduce the charge current in the writing process by using high performance spin Hall material, the size of driving transistors can be minimized and the bit density can be increased. With these advantages, SOT-MRAM has become very attractive as a promising candidate for the third generation MRAM with fast writing, low writing energy and high bit density. Since the spin Hall angle θ_{SH} can be tailored by implementing suitable materials, there are huge efforts in exploring a large spectrum of materials and their spin-related transport properties in order to maximum the performance of SOT-MRAM.

3. Topological insulator – the key material

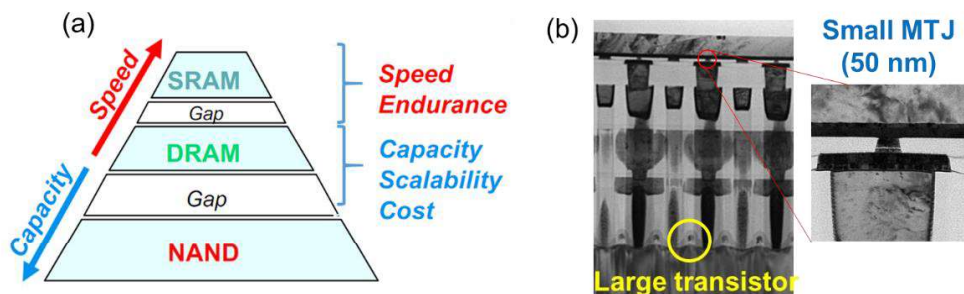


Figure 4. (a) The memory gaps in conventional memories. The gaps between SRAM, DRAM, and NAND show the positions that STT-MRAM can fill. (b) TEM image of a STT-MRAM device. High writing current is the most disadvantage feature of STT-MRAM. This requires large driving transistors and make it difficult to increase the bit density of MRAM. Courtesy by L Thomas et al., MSST 2017.

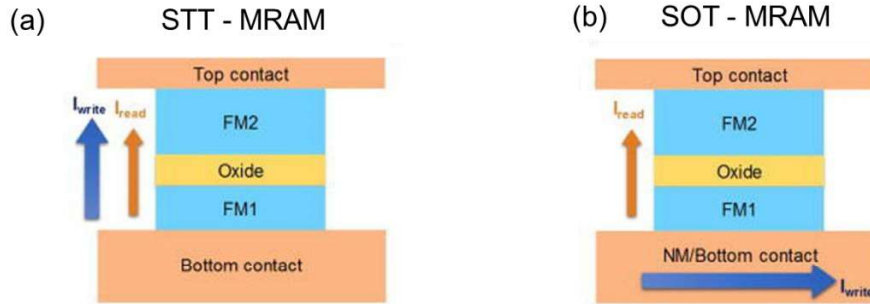


Figure 5. Difference in writing mechanism of (a) STT-MRAM and (b) SOT-MRAM. The pure spin current in SOT-MRAM is generated by the spin Hall effect from an in-plane charge current (blue arrow). This spin current flows upward into the free layer and flips its magnetization. © (2018) reprinted with permission from the American Institute of Physics.

Recently, both theories and experiments have found out there are some exotic materials with insulating bulk but topologically protected conducting surface / edge states, as shown in Fig. 6(a). These materials are called topological insulators (TIs) [19]. These surface states have a unique property, called spin-momentum locking, as shown in Fig. 6(b). Therefore, back-scattering is prohibited if spin is conserved, resulting in high surface electron mobility. Furthermore, these surface states have Dirac-like dispersion, which can result in a large spin Hall angle from the Berry phase effect. These characteristics make TIs a very hot topic in spintronics, which may become a key material for future spintronic devices.

In 2007, M. König *et al.* experimentally observed the spin polarized edge states in a HgTe quantum well, which is a 2D TI, 20 years after the conceptual proposal of topology in condensed matter physics independently by D. J. Thouless, F. D. M. Haldane and J. M. Kosterlitz, who were honored with the Physics Nobel Prizes in 2016 [20]. Then, 3D TIs were soon discovered in several Bi-based V-VI compounds, such as Bi₂Se₃ and (Bi_{0.5}Sb_{0.5})₂Te₃, followed by the discovery of their giant spin Hall angle [21-22]. Their spin Hall angles are at least one order of magnitude larger than those of heavy metals, anti-ferromagnets or oxide materials. That means TIs can provide much higher charge-to-spin conversion efficiency than other

spin source materials. Figure 7(a) compares the power consumption of SOT switching by using TIs and heavy metals as the spin source. TIs can reduce the power consumption down to less than 25% of heavy metals [23]. These results make TIs a very hot topic in spintronics.

However, TIs have a fundamental problem due to their insulating nature. In Bi-based V-VI compound TIs, due to their large band-gap and low carrier mobility, the conductivity σ of those TIs is limited to $\sim 10^4 \Omega^{-1}\text{m}^{-1}$, which is much lower than that of typical metallic ferromagnets ($\sim 6 \times 10^5 \Omega^{-1}\text{m}^{-1}$) used in MRAM. This causes a serious problem for TIs as spin Hall materials. As illustrated in Fig. 7(b), when attached to a metallic ferromagnet, most of the charge current is shunted through the magnetic recording layer and does not contribute to generation of pure spin current in the spin Hall layer. Exploring new TI materials with both high conductivity and strong spin Hall effect is essential to realize realistic applications of TIs to SOT-MRAM.

4. BISB – a conductive TI and its application to SOT-MRAM

Among various TI materials, Bi_{1-x}Sb_x emerges as a unique TI with a narrow band gap (bulk band gap < 20 meV), which is much smaller the band gap of other TIs such as Bi₂Se₃ (~ 300 meV) or Bi₂Te₃ (~ 130 meV) [24]. More importantly, Bi_{1-x}Sb_x shows higher carrier mobility ($\sim 10^4$ cmV⁻¹s⁻¹), and its bulk conductivity is as high as $4 \times 10^5 \sim 6.4 \times 10^5 \Omega^{-1}\text{m}^{-1}$, compatible to other metallic materials used in realistic MRAM. Recently, we have developed epitaxial growth technique for high quality BiSb thin films using molecular beam epitaxy (MBE) and obtained $\sigma = 4 \times 10^5 \sim 6 \times 10^5 \Omega^{-1}\text{m}^{-1}$ for BiSb thin films thicker than 80 nm, and $\sigma = 1 \times 10^5 \sim 4 \times 10^5 \Omega^{-1}\text{m}^{-1}$ (average $\sigma \sim 2.5 \times 10^5 \Omega^{-1}\text{m}^{-1}$) for BiSb thin films thinner than 25 nm as show in Fig. 8(a) [25]. Meanwhile, the topologically protected surface states of Bi_{1-x}Sb_x ($0.07 \leq x \leq 0.22$) were confirmed by angle-resolved photoemission spectroscopy (ARPES) measurements, as shown in

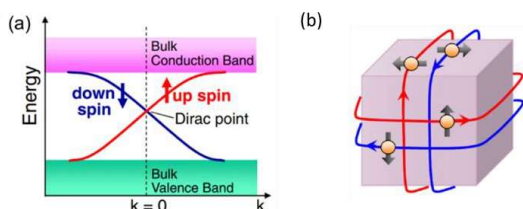


Figure 6. (a) Energy dispersion of the spin non-degenerate edge states in a 2D TI, which resembles an 1D Dirac cone. (b) Schematic real-space image of 2D helical surface states of 3D TI. © (2013) reprinted with permission from the Physical Society of Japan.

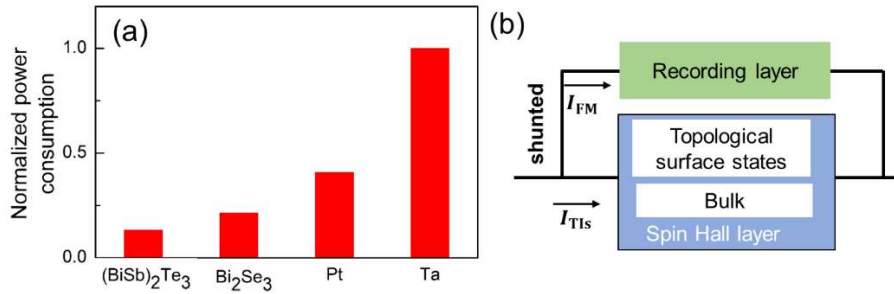


Figure 7. Normalized power consumption (with Ta set to be unity) for SOT switching using $(\text{BiSb})_2\text{Te}_3$, Bi_2Se_3 , Pt and Ta © (2017) reprinted with permission from the American Physical Society. (b) Current shunting effect due to the low electrical conductivity of TIs.

Fig. 8(b) [26-28].

Furthermore, we observed a giant spin Hall angle of $\theta_{\text{SH}} \sim 52$ even at the room temperature in BiSb/MnGa bilayers, and make BiSb the best candidate for the spin current source in ultra-low power SOT-MRAM. Table 1 compares the electrical conductivity σ , spin Hall angle θ_{SH} , and spin Hall conductivity $\sigma_{\text{SH}} = (\hbar/2e)\theta_{\text{SH}} \times \sigma$. As shown in Table 1, BiSb achieves the largest θ_{SH} , and outperforms other spin source materials by at least an order of magnitude in term of σ_{SH} .

Figure 9(a) shows room-temperature spin-orbit torque (SOT) switching in BiSb/MnGa bilayer at a low critical current density J_{sw} of $1.5 \times 10^6 \text{ A/cm}^2$, even though the MnGa ferromagnet show very large anisotropy field. Note that other spin source materials require much higher switching current density in junctions with MnGa, such as Ta ($J_{\text{sw}} \sim 110 \times 10^6 \text{ A/cm}^2$), Pt ($J_{\text{sw}} \sim 50 \times 10^6 \text{ A/cm}^2$) or antiferromagnet like IrMn ($J_{\text{sw}} \sim 150 \times 10^6 \text{ A/cm}^2$) [31]. Figure 9(b) projects the performance of BiSb-based SOT-MRAM with STT-MRAM at the same size of 37 nm. The writing current can be reduced by at least an order of magnitude, while the writing speed is 20~50 times faster. Thus, the writing energy can be reduced by at least two orders of magnitude. Moreover, the low

writing current requires smaller driving transistors, which helps increase the bit density of SOT-MRAM [32-33]. These demonstrated that BiSb-based SOT-MRAM outperforms STT-MRAM and can replace conventional volatile memory technologies, such as DRAM and SRAM.

Table 1. Room-temperature spin Hall angle θ_{SH} , conductivity σ , and spin Hall conductivity σ_{SH} of several heavy metals and TIs.

	θ_{SH}	σ ($\Omega^{-1}\text{m}^{-1}$)	σ_{SH} ($\hbar/2e \Omega^{-1}\text{m}^{-1}$)
β -Ta	0.15	5.3×10^5	0.8×10^5
β -W	0.4	4.7×10^5	1.9×10^5
Pt	0.08	4.2×10^6	3.4×10^5
Bi_2Se_3	2-3.5	5.7×10^4	$1.1\text{-}2.0 \times 10^5$
$\text{Bi}_x\text{Se}_{1-x}$	18.8	7.8×10^3	1.47×10^5
$\text{Bi}_{0.9}\text{Sb}_{0.1}$ (this work)	52	2.5×10^5	1.3×10^7

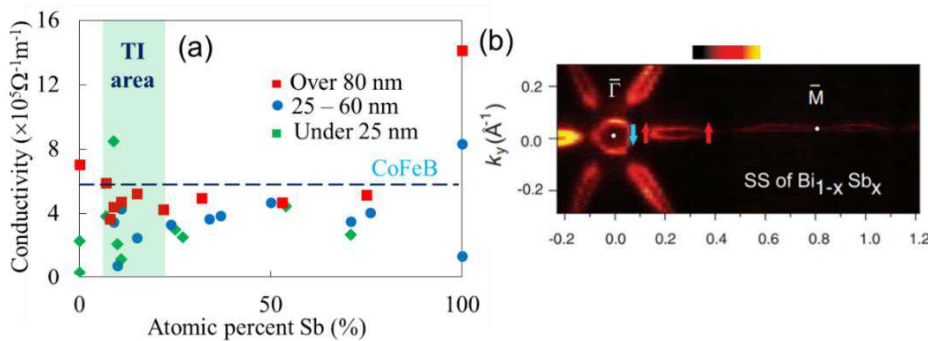


Figure 8. (a) Electrical conductivity at 270 K of various $\text{Bi}_{1-x}\text{Sb}_x$ samples with different Sb concentration and thickness (c) (2017) reprinted with permission from the American Institute of Physics. (b) ARPES intensity map of surface states in $\text{Bi}_{0.91}\text{Sb}_{0.09}$. Arrows indicate spin direction. © (2009) reprinted with permission from American Association for the Advancement of Science.

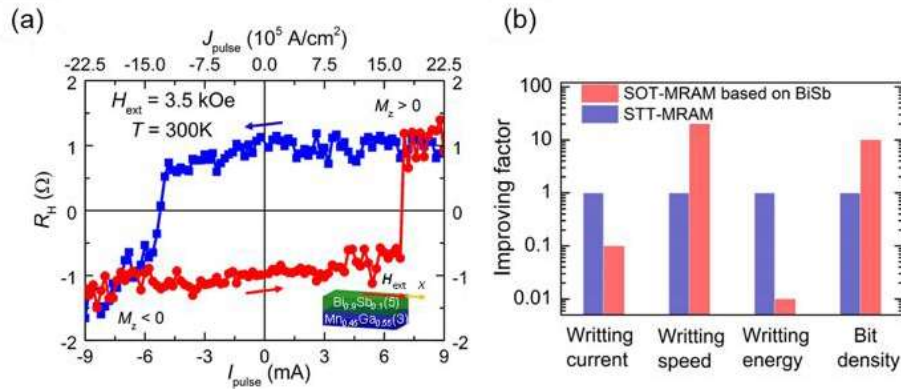


Figure 9. (a) Room-temperature current induced magnetization switching in the $Bi_{0.9}Sb_{0.1}$ (5 nm) / $Mn_{0.45}Ga_{0.55}$ (3 nm) bilayer under 100 ms pulse currents and an in-plane magnetic field H_{ext} of +3.5 kOe © (2018) reprinted with permission from Springer Nature. (b) Benchmarking of SOT-MRAM with BiSb as a spin source, compared with STT-MRAM with the same size of 37 nm.

Note that these samples are grown on GaAs substrates by the ultra-precise MBE method to achieve excellent crystal quality. However, the MBE technique is incompatible with mass production. Meanwhile, physical vapor deposition (PVD) techniques such as magnetron sputtering are commonly used in industrial memory and logic fabrication process. Therefore, it is essential to evaluate the performance of BiSb deposited by PVD for realistic BiSb-based spintronic applications, especially for ultralow-power SOT-MRAM.

Very recently, we have used magnetron sputtering to deposit BiSb, and confirm that the spin Hall angle of BiSb is still large enough for practical applications [34]. Figure 10(a-b) show the SOT induced magnetization switching by DC current and pulse current in CoTb (2.7 nm)/Pt (1 nm)/BiSb (10 nm) stack structure fabricated by magnetron sputtering on silicon substrates. One can see that the critical switching current can be as low as 4×10^5 A/cm² at $H_x = 500$ Oe for DC current and 6×10^6 A/cm² at pulse width of 50 ns. These values are at least an order smaller than those in heavy metals ($\sim 10^7$ A/cm² for DC current and $\sim 10^8$ A/cm² for pulse current) [35-37]. Indeed, the effective spin Hall angle in these samples is estimated around 1.2 which is still much larger than other spin sources as we know so far. Considering the low spin transmittance of the CoTb interface and spin loss in the Pt (1 nm) interlayer, the intrinsic spin Hall angle of BiSb in these samples is 8. As shown in Fig. 10(c), in term of power consumption, the performance of BiSb fabricated by sputtering technique (green column) is still at least an order smaller than in heavy metals and other TIs. These results reconfirmed the advantage of BiSb as the spin source for SOT-MRAM. As over ten years have passed since the proposals and experimental realization of TIs, BiSb emerges as the most promising candidate for the first industrial applications of TIs.

5. Other novel spin-dependent transport phenomena in BiSb-ferromagnet bilayers

Exotic spin-dependent phenomena of TIs, BiSb in particular, are not limited to the spin Hall effect and applications to SOT-MRAM. We observed many other novel effects which can be applied to various spintronic device applications. For example, we observed a giant unidirectional spin Hall magnetoresistance (USMR) in GaMnAs / polycrystalline BiSb heterostructures, where the USMR ratio can reach 1.1% which is larger than those in metallic bilayers and other TI / metallic ferromagnet

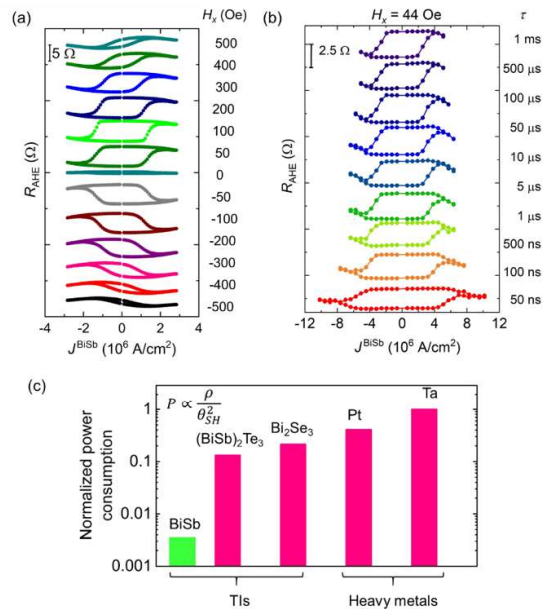


Figure 10. (a) SOT magnetization switching in CoTb (2.7 nm)/Pt (1 nm)/BiSb (10 nm) stack measured by DC current at different H_x . (b) Pulse-current induced SOT magnetization switching in CoTb (2.7 nm)/Pt (1 nm)/BiSb (10 nm) stack at various pulse widths τ down to 50 ns and $H_x = 44$ Oe. (c) Normalized power consumption (with Ta set to be unity) for SOT switching using BiSb, $(BiSb)_2Te_3$, Bi_2Se_3 , Pt and Ta.

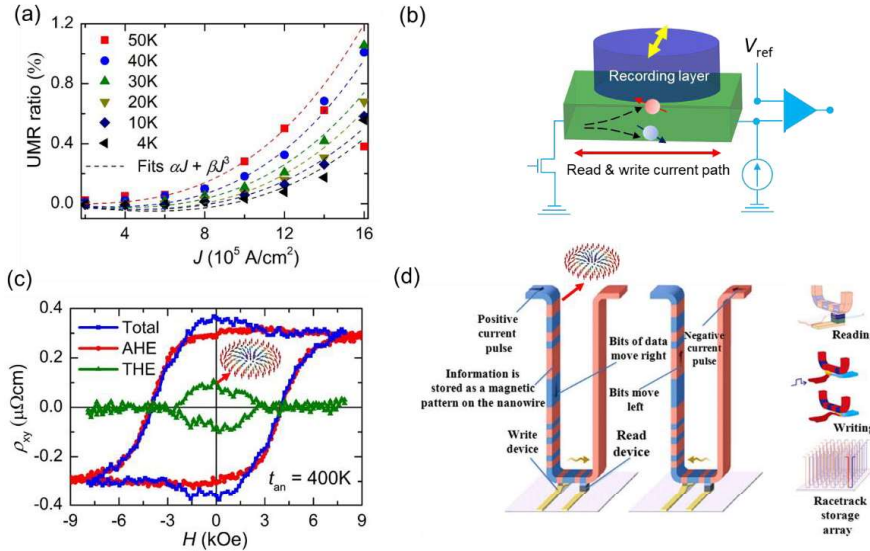


Figure 11. (a) USMR ratio in GaMnAs (10 nm)/BiSb (10 nm) measured at different temperature. (b) Two-terminal planar MRAM device with an extremely simple stacking structure, consisting of only a ferromagnetic layer and a spin Hall layer. SOT and USMR are utilized for data writing and reading, respectively. (c) Evidence of Néel-type skyrmions detected at room temperature by the topological Hall effect (THE) (green lines), extracted from the total Hall effect (blue lines) and the anomalous Hall effect (AHE) (red lines) in MnGa(5 nm)/BiSb(10 nm) bilayers. (d) Application of skyrmions to racetrack memory in an array of U-shaped magnetic nanowires © (2008) reprinted with permission from American Association for the Advancement of Science.

systems by several orders of magnitude, as shown in Fig. 11(a) [38]. We found that the main mechanism of this giant USMR effect in this heterostructure is magnon absorption/emission and strong spin-disordering scattering in the GaMnAs layer. These results can be used to significantly simplify the structure of SOT-MRAM. Figure 11(b) illustrates a two-terminal planar MRAM device with an extremely simple stacking structure, consisting of only a ferromagnetic layer and a spin Hall layer. In this device, SOT and USMR are utilized for data writing and reading, respectively. Moreover, since the magnon scattering rate increases at high temperature, using Fe-doped narrow-gap ferromagnetic semiconductors with room-temperature ferromagnetism, such as GaFeSb or InFeSb, may improve the USMR ratio to over 10%, which is essential for USMR-MRAM with extremely simple structure and fast writing/reading.

Observation of skyrmions by the topological Hall effect (THE) is another novel phenomenon. Figure 11(c) shows THE (green line) observed at room temperature even without an external magnetic field, demonstrating field-free ground-state skyrmions [39]. A large critical interfacial DMI constant of 5.1 pJ/m was observed. These results confirm that BiSb topological insulator can generate not only colossal spin-orbit torque, but also giant interfacial Dzyaloshinskii-Moriya-Interaction (DMI) for generation and manipulation of skyrmions. This giant SOT and DMI can be used in the skyrmion or chiral

domain wall racetrack memory as shown Fig. 11(d). One unique characteristic of racetrack memory is its 3D structure. A racetrack memory [40] can use hundreds of millions of U-shaped nanowires arranged vertically like a forest in a very small area size. This characteristic allows racetrack memory to store a vast amounts of data, and makes racetrack memory become a very attractive memory.

While more efforts are required to integrate BiSb to realistic spintronic device, our results have open the dawn of a new era of ultralow power and fast TI-based spintronics.

Acknowledgments

This work is supported by JST-CREST (JPMJCR18T5), and partly by TDK corporation. N.H.D.K. acknowledges Marubun Research Promotion Foundation for an exchange research grant, and JSPS for a postdoctoral fellowship for research in Japan (P20050). This work was done with collaboration from Y. Ueda, K. Yao, S. Nakano, T. Shirokura of Tokyo Tech., and Y. Miyamoto of NHK.

References

- [1] Bardeen, J. W. and Brattain, W. H. The Transistor, A Semi-Conductor Triode, *Phys. Rev.*, **74**, 230-231 (1948).
- [2] Moore, G. E. Cramming More Components Onto Integrated Circuits, *Proc. IEEE*, **86**, 82-85 (1998).
- [3] Wolf, S. A., Awschalom, D. D., Buhrman, R. A., Daughton, J. M., von Molnár, S., Roukes, M. L.,

- Chtchelkanova, A. Y. and Treger, D. M. Spintronics: A Spin-Based Electronics Vision for the Future, *Science*, **294**, 1488-1495 (2001).
- [4] Akinaga, H. and Ohno, H. Semiconductor spintronics, *IEEE Trans. Nanotech.*, **1**, 19-31 (2002).
- [5] Žutić, I., Fabian, J. and Sarma, S. D. Spintronics: Fundamentals and applications, *Rev. Mod. Phys.* **76**, 323-410 (2004).
- [6] Ando, Y. Spintronics technology and device development, *Jpn. J. Appl. Phys.*, **54**, 070101 (2015).
- [7] Tehrani, S., Slaughter, J. M., Deherrera, M., Engel, B. N., Rizzo, N. D., Salter, J., Durlam, M., Dave, R. W., Janesky, J., Butcher, B., Smith, K. and Grynkewich, G. Magnetoresistive random access memory using magnetic tunnel junctions, *Proc. IEEE*, **91**, 703-714 (2003).
- [8] Slonczewski, J. C. J. Magn. Current-driven excitation of magnetic multilayers, *Magn. Mater.*, **159**, L1-L7 (1996).
- [9] Berger, L. Emission of spin waves by a magnetic multilayer traversed by a current, *Phys. Rev. B*, **54**, 9353-9358 (1996).
- [10] Tsoi, M., Jansen, A. G. M., Bass, J., Chiang, W. C., Seck, M., Tsoi, V., and Wyder, P. Excitation of a Magnetic Multilayer by an Electric Current, *Phys. Rev. Lett.*, **80**, 4281-4284 (1998).
- [11] Wegrove, J. E., Kelly, D., Guitienne, P., Jaccard, Y. and Ansermet, J. P. Current-induced magnetization reversal in magnetic nanowires, *Europhys. Lett.*, **45**, 626-632 (1999).
- [12] Myers, E. B., Ralph, D. C., Katine, J. A., Louie, R. N. and R. A. Buhrman. Current-Induced Switching of Domains in Magnetic Multilayer Devices, *Science*, **285**, 867-870 (1999).
- [13] Edelstein, V. M. Spin polarization of conduction electrons induced by electric current in two-dimensional asymmetric electron systems, *S. S. Comm.*, **73**, 233-235 (1990).
- [14] Chernyshov, A., Overby, M., Liu, X., Furdyna, J. K., Geller, Y. L. and Leonid, P. R. Evidence for reversible control of magnetization in a ferromagnetic material by means of spin-orbit magnetic field, *Nat. Phys.*, **5**, 656-659 (2009).
- [15] Kato, Y. K., Myers, R. C., Gossard, A. C. and Awschalom, D. D. Observation of the Spin Hall Effect in Semiconductors, *Science*, **306**, 1910-1913 (2004).
- [16] Ramaswamy, R., Lee, J. M., Cai, K. and H. Yang, Recent advances in spin-orbit torques: Moving towards device applications, *Appl. Phys. Rev.*, **5**, 031107 (2018).
- [17] Sinova, J. and Jungwirth, T. Surprises from the spin Hall effect, *Phys. Today* **70**, 38-42 (2017).
- [18] Meena, J. S., Sze, S. M., Chand, U. and Tseng, T. Y. Overview of emerging nonvolatile memory technology, *Nano. Re. Lett.*, **9**, 526 (2014).
- [19] Ando, Y. Topological Insulator Materials, *J. Phys. Soc. Jpn.*, **82**, 102001 (2013).
- [20] König, M., Wiedmann, S., Brüne, C., Roth, A., Buhmann, H., Molenkamp, L. W., Qi, X. L. and Zhang, S. C. Quantum spin hall insulator state in HgTe quantum wells, *Science*, **318**, 766 (2007).
- [21] Mellnik, A. R., Lee, J. S., Richardella, A., Grab, J. L., Mintun, P. J., Fischer, M. H., Vaezi, A., Manchon, A., Kim, E. A., Samarth, N., and Ralph, D. C. Spin-transfer torque generated by a topological insulator, *Nature*, **511**, 449 (2014).
- [22] Fan, Y., Upadhyaya, P., Kou, X., Lang, M., Takei, S., Wang, Z., Tang, J., He, L., Chang, L. T., Montazeri, M., Yu, G., Jiang, W., Nie, T., Schwartz, R. N., Tserkovnyak, Y. and Wang, K. L. Magnetization switching through giant spin-orbit torque in a magnetically doped topological insulator heterostructure, *Nat. Mater.*, **13**, 699-704 (2014).
- [23] Han, J., Richardella, A., Siddiqui, S. A., Finley, J., Samarth, N. and Liu, L. Room-Temperature Spin-Orbit Torque Switching Induced by a Topological Insulator, *Phys. Rev. Lett.*, **119**, 077702 (2017).
- [24] Teo, J. C. Y., Fu, L. and Kane, C. L. Surface states and topological invariants in three-dimensional topological insulators: Application to Bi_{1-x}Sb_x, *Phys. Rev. B*, **78**, 045426 (2008).
- [25] Ueda, Y., Khang, N. H. D., Yao, K. and Hai, P. N. Epitaxial growth and characterization of Bi_{1-x}Sb_x spin Hall thin films on GaAs(111)A substrates, *Appl. Phys. Lett.* **110**, 062401 (2017).
- [26] Hsieh, D., Xia, Y., Wray, L., Qian, D., Pal, S., Dil, J. H., Osterwalder, J., Meier, F., Bihlmayer, G., Kane, C. L., Hor, Y. S., Cava, R. J. and Hasan, M. Z. Observation of Unconventional Quantum Spin Textures in Topological Insulators, *Science*, **323**, 919-922 (2009).
- [27] Hirahara, T., Sakamoto, Y., Saisyu, Y., Miyazaki, H., Kimura, S., Okuda, T., Matsuda, I. Topological metal at the surface of an ultrathin Bi_{1-x}Sb_x alloy film, *Phys. Rev. B*, **81**, 165422 (2010).
- [28] Nishide, A., Taskin, A. A., Takeichi, Y., Okuda, T., Kakizaki, A., Hirahara, T., Nakatsuji, K., Komori, F., Ando, Y. and Matsuda, I. Direct mapping of the spin-filtered surface bands of a three-dimensional quantum spin Hall insulator, *Phys. Rev. B*, **81**, 041309(R) (2010).
- [29] Taskin, A. A. and Ando, Y. Quantum oscillations in a topological insulator Bi_{1-x}Sb_x, *Phys. Rev. B*, **80**, 085303 (2009).
- [30] Taskin, A. A., Segawa, K. and Ando, Y. Oscillatory angular dependence of the magnetoresistance in a topological insulator Bi_{1-x}Sb_x, *Phys. Rev. B*, **82**, 121302 (R) (2010).

- [31] Meng, K. K., Miao, J., Xu, X. G., Wu, Y., Zhao, X. P., Zhao, J. H. and Jiang, Y. Anomalous Hall effect and spin-orbit torques in MnGa/IrMn films: modification from strong spin Hall effect of the antiferromagnet, *Phys. Rev. B*, **94**, 214413 (2016)
- [32] Khang, N. H. D., Ueda, Y. and Hai, P. N. A conductive topological insulator with large spin Hall effect for ultralow power spin-orbit torque switching, *Nat. Mater.*, **17**, 808 (2018).
- [33] Hai, P. N., Khang, N. H. D., Yao, K. and Ueda, Y. Conductive BiSb topological insulator with colossal spin Hall effect for ultra-low power spin-orbit-torque switching, *Proc. SPIE* **10732**, 107320U (2018).
- [34] Khang, N. H. D., Nakano, S., Shirokura, T., Miyamoto, Y., Hai, P. N. Ultralow power spin-orbit torque magnetization switching induced by a non-epitaxial topological insulator on Si substrates, *Sci. Rep.*, **10**, 12185 (2020).
- [35] Liu, L., Pai, C. F., Li, Y., Tseng, H. W., Ralph, D. C., Buhrman, R. A. Spin-torque switching with the giant spin Hall effect of tantalum, *Science*, **336**, 555–558 (2012).
- [36] Liu, L., Lee, O. J., Gudmundsen, T. J., Ralph, D. C. and Buhrman, R. A. Current-induced switching of perpendicularly magnetized magnetic layers using spin torque from the spin Hall effect, *Phys. Rev. Lett.*, **109**, 096602 (2012).
- [37] Hao, Q. and Xiao, G. Giant spin Hall effect and switching induced by spin-transfer torque in a W/Co40Fe40B20/MgO structure with perpendicular magnetic anisotropy, *Phys. Rev. Appl.*, **3**, 034009 (2015).
- [38] Khang, N. H. D. and Hai, P. N. Giant Unidirectional Spin Hall Magnetoresistance in topological insulator-ferromagnetic semiconductor heterostructures, *J. Appl. Phys.*, **126**, 233903 (2019).
- [39] Khang, N. H. D., Fan, T. and Hai, P. N. Zero-field topological Hall effect as evidence of ground-state skyrmions at room temperature in BiSb/MnGa bilayers, *AIP Adv.* **9**, 125309 (2019).
- [40] Meena, J. S., Sze, S. M., Chand, U. and Tseng, T. Y. Overview of emerging nonvolatile memory technologies, *Nano. Re. Lett.* **9**, 526 (2014).